Theory of Hierarchical Lamellar Structures from $A(BC)_nBA$ Multiblock Copolymers

Weihua Li*

The Key Laboratory of Molecular Engineering of Polymers, Ministry of Education, Department of Macromolecular Science, Fudan University, Shanghai 200433, China

An-Chang Shi†

Department of Physics and Astronomy, McMaster University, Hamilton, Ontario, Canada, L8S 4M1

Received July 22, 2008; Revised Manuscript Received December 3, 2008

ABSTRACT: The phase behavior of $A(BC)_nBA$ multiblock copolymer melts is investigated using self-consistent mean-field theory (SCMFT). Solutions of the SCMFT equations corresponding to hierarchical lamellar structures are obtained. The free energy of these structures are used to construct phase diagrams. It is predicted that hierarchical lamellar structures with different number of "internal" BC layers can be formed. The number of BC layers of the stable lamellar structure is determined by the competition between chain entropy and interfacial energy. It is found that more BC layers are preferred when the interactions between A and BC blocks are much stronger than that between B and C blocks.

I. Introduction

Block copolymers have been studied intensively in the past decades due to the fact that these materials can self-assemble into a variety of ordered structures with characteristic lengths determined by the copolymer size.[1,2] For the simplest case of AB diblock copolymers, it has been well established that they can form spherical, cylindrical, gyroid, and lamellar phases.[3] When the number of distinct blocks is increased from two, the complexity and variety of self-assembled structures are significantly increased.[4,5] In particular, it has been shown experimentally and theoretically that a simple extension of AB diblock copolymers to ABC triblock copolymers leads to a very large number of new morphologies.[4,6,7] Recent development of polymer chemistry enables the synthesis of more complex block copolymers. Self-assembly of these multiblock copolymer opens the door of engineering novel structures. Due to the complexity of the block copolymers and their self-assembled structures, understanding the phase behavior of multiblock copolymers presents a challenging theoretical problem.

Recently a new type of multiblock copolymers, composed of one or two long tails and many short midblocks, have been synthesized. The phase behavior of this class of block copolymers have attracted increasing attention.[5,8,9] In the experiments carried out by Matsushita's group, hierarchical lamellar structures with double periods are observed in $A(BA)_nBA$ and $A(BC)_nBA$ linear multiblock copolymers. In the first example, multiblock copolymers of the SISISISISIS type, having two long polystyrene (S) tail blocks and nine short polystyrene (S) and polyisoprene (I) middle blocks, were examined.[8] The lamellar structures formed by this multiblock copolymer is composed of one thick S layer and one ISI three-layered lamella, although the morphologies are with poor long-range order. In the second type of multiblock copolymers (PISISISISIP), the two end blocks are replaced by blocks different from the I and S blocks. Well ordered lamellar structures are obtained in this system.[9] The hierarchical lamellae include one thick P layer and five thin ISISI layers. Generically these two types of multiblock copolymers can be expressed as $A(BC)_nBA$, where n is the repeating number of alternative BC short blocks. For a given n, a number of hierarchical lamellar structures with different number of thin-layers are possible. For example, for the case of $n = 4$, the number of thin-layers can be 1, 3, 5, 7 and 9. In ref 9, a simple argument is used to explain the stable lamellar structure for a given n. This is done by counting the possible molecular-configurations in each structure. Because the number of molecular-configurations is related to entropic contribution to the free energy, it is reasonable to argue that the stable structure is the one with the largest number of configurations. Indeed this argument seems to be able to account for the observations in ref 9. However, this simple counting model ignores the interfacial energy, as well as the entropy of chain stretching. One would expect that these factors will have a large effect on the phase behavior. Therefore, it is desirable to carry out a systematical study of the systems.

Theoretically the formation of hierarchical lamellar phases has been studied by ten Brinker and co-workers.[10−12] First of all, multiblock copolymers of the type $A_m(BA)_n$, consisting of a long A block connected to a $(BA)_n$ multiblocks, is investigated by using the self-consistent mean-field theory (SCMFT).[10,11] The formation of hierarchical lamellar phases with two length scales is demonstrated in these studies.[10] It is observed that the formation of the long-period A−BA microphases occurs first when the interaction between A and B blocks is increased, the short length scale structure is formed inside the domains of the large scale one as the interaction is further increased. The period of the structures depends on the interaction parameter. In a subsequent study from the same group,[11] the same type of multiblock copolymer is re-examined. Hierarchical lamellar structure with seven thin-layers is observed as a stable structure for $A_{20}(BA)_{10}$ by comparing its free energy with those of other possible lamellar structures. Motivated by the experiments of,[9] Subbotin, Klymko and ten Brinke have investigated the self-assembly of $A(BC)_nBA$ multiblock copolymers using a strong segregation theory. The free energy per multiblock copolymer is estimated by considering the contributions from the different ways of creating specific sequences of loops and bridges. For multiblock copolymers of the type $A(BC)_nBA$, these authors predicted a number of stable hierarchical lamellar phases. Despite these previous theoretical studies, a comprehensive

---

* Corresponding author. E-mail: weihuali@fudan.edu.cn.

† E-mail: shi@mcmaster.ca.

10.1021/ma801651u CCC: $40.75

theoretical study on the formation of hierarchical lamellae in A(BC)$_n$BA is still lacking.

In A(BA)$_n$BA or A(BC)$_n$BA multiblock copolymers, lamellar structures are formed when the volume fraction of the two end A blocks is about $^1/_2$. In these lamellar structures, the two end A blocks form one layer whereas the BC blocks form the other layer. When the repulsive interaction between the B and C blocks is strong enough, BC blocks will undergo microphase separation, forming hierarchical lamellar structures if the volume fractions of B and C blocks are similar. Because the B and C blocks are confined in the BC layer, the B phase separation may be viewed as a self-assembly process in a confined geometry. In particular, for the A(BC)$_n$BA copolymers, the incompatibility between the A block and the BC blocks leads to a tighter confinement as compared with the case of A(BA)$_n$BA copolymers. In general, structural formation of block copolymer microphases is determined by the competition between the chain entropy and interfacial energy. For the case of diblock copolymer melts, the chain entropy is largely determined by the chain stretching, which can be estimated using the strong segregation theory.[13] For the multiblock copolymers, the chain entropy is not only related with the stretching energy, but also with the ways in which the polymer chains are arranged in the different domains. This configurational entropy is the base of the counting model in ref 9.

In this paper we present a study of the phase behavior of A(BC)$_n$BA multiblock copolymers. In order to calculate the free energy of a hierarchical lamellar structure accurately, we employ the self-consistent mean-field theory (SCMFT) in our study. SCMFT is a theoretical framework which is capable to connect molecular architecture and composition to equilibrium ordered phases.[14,15] In our study, solutions of SCMFT equations corresponding to hierarchical lamellar structures with different number of BC layers are obtained. Comparison of the free energy density of these phases leads to the construction of phase diagrams of the multiblock copolymers. The phase diagrams reveal that lamellar structures with different number of BC-layers can exist for a fixed value of n. The stability of these different lamellar phases depend on the AB, BC and CA interactions.

II. Self-Consistent Mean-Field Theory of Multiblock Copolymers

We use a canonical ensemble and consider an incompressible melt of block copolymers in a volume V. The block copolymers are A(BC)$_n$BA-type multiblock copolymers. The two tail A blocks are assumed to have equal length, whereas the middle blocks contain $n + 1$ B blocks and n C blocks. For a block copolymer with a degree of polymerization N, the chain lengths of the A, B and C blocks are f_AN, f_BN, and f_CN ($f_A + f_B + f_C = 1$), respectively. For simplicity, we assume that the B and C blocks have equal lengths specified by $\Delta f_B = f_B/(n + 1)$ and $\Delta f_C = f_C/n$. All spacial lengths are expressed in units of the radius of gyration, $R_g = a\sqrt{N/6}$, of the copolymer, where a is the statistical segment length which is assumed to be the same for the different type of monomers. Within the SCMFT the free-energy F of n_c multiblock copolymer chains in the volume is given by,[14,15]

$$\frac{F}{n_c k_B T} = -\ln Q + \frac{1}{V}\int \mathrm{d}\mathbf{r}\ \{\chi_{AB}N\varphi_A(\mathbf{r})\varphi_B(\mathbf{r}) + \chi_{AC}N\varphi_A(\mathbf{r})\varphi_C(\mathbf{r}) + \chi_{BC}N\varphi_B(\mathbf{r})\varphi_C(\mathbf{r}) - \omega_A(\mathbf{r})\varphi_A(\mathbf{r}) - \omega_B(\mathbf{r})\varphi_B(\mathbf{r}) - \omega_C(\mathbf{r})\varphi_C(\mathbf{r})\}, \quad (1)$$

where T is the temperature, k_B is the Boltzmann constant. ϕ_A, ϕ_B, and ϕ_C are the spatially varying monomer concentrations and ω_A, ω_B, and ω_C are the corresponding conjugate fields. Q is the partition function of a single copolymer chain in the mean fields ω_A, ω_B. and ω_C. The interactions between the different monomers are described using three Flory−Huggins interaction parameters, χ_{AB}, χ_{AC}, and χ_{BC}. The SCMFT equations are obtained by minimizing the free energy specified in eq 1 with respect to the monomer concentrations and the fields. Carrying out such a minimization leads to the following SCMFT equations,

$$\begin{aligned}
\omega_A(\mathbf{r}) &= \chi_{AB}N\varphi_B(\mathbf{r}) + \chi_{AC}N\varphi_C(\mathbf{r}) + \eta(\mathbf{r})\\
\omega_B(\mathbf{r}) &= \chi_{AB}N\varphi_A(\mathbf{r}) + \chi_{BC}N\varphi_C(\mathbf{r})\eta(\mathbf{r})\\
\omega_C(\mathbf{r}) &= \chi_{AC}N\varphi_A(\mathbf{r}) + \chi_{BC}N\varphi_B(\mathbf{r}) + \eta(\mathbf{r})\\
\varphi_A(\mathbf{r}) &= \frac{1}{Q}\int_0^{f_A/2} \mathrm{d}s\ q(\mathbf{r},s)q^\dagger(\mathbf{r},s) + \frac{1}{Q}\int_{1-f_A/2}^{1} \mathrm{d}s\ q(\mathbf{r},s)q^\dagger(\mathbf{r},s)\\
\varphi_B(\mathbf{r}) &= \sum_{i=0}^{n} \frac{1}{Q}\int_{f_A/2+i(\Delta f_B+\Delta f_C)}^{f_A/2+i(\Delta f_B+\Delta f_C)+\Delta f_B} \mathrm{d}s\ q(\mathbf{r},s)q^\dagger(\mathbf{r},s)\\
\varphi_C(\mathbf{r}) &= \sum_{j=0}^{n-1} \frac{1}{Q}\int_{f_A/2+j(\Delta f_B+\Delta f_C)+\Delta f_B}^{f_A/2+(j+1)(\Delta f_B+\Delta f_C)} \mathrm{d}s\ q(\mathbf{r},s)q^\dagger(\mathbf{r},s).
\end{aligned} \quad (2)$$

The single-chain partition function Q is given by

$$Q = \frac{1}{V}\int \mathrm{d}^3\mathbf{r}\ q(\mathbf{r},s)q^\dagger(\mathbf{r},s). \quad (3)$$

The concentrations must satisfy the incompressibility condition,

$$\varphi_A(\mathbf{r}) + \varphi_B(\mathbf{r}) + \varphi_C(\mathbf{r}) = 1. \quad (4)$$

The incompressibility condition is enforced *via* the Lagrange multiplier $\eta(\mathbf{r})$.

A very important property of the polymers is the probability distribution of the chain conformations. This property can be described by the function $q(\mathbf{r}, s)$, which is the probability that a polymer chain segment at contour length s and locate at position $\mathbf{r}$. This distribution function and its conjugate, $q^\dagger(\mathbf{r}, s)$, satisfy the modified diffusion equations:[15]

$$\begin{aligned}
\frac{\partial q(\mathbf{r},s)}{\partial s} &= \nabla^2 q(\mathbf{r},s) - w(\mathbf{r},s)q(\mathbf{r},s)\\
-\frac{\partial q^\dagger(\mathbf{r},s)}{\partial s} &= \nabla^2 q^\dagger(\mathbf{r},s) - w(\mathbf{r},s)q^\dagger(\mathbf{r},s),
\end{aligned} \quad (5)$$

where the "time"-dependent fields $w(\mathbf{r}, s)$ are specified by (for $0 \le i \le n$ and $0 \le j < n$),

$$\omega(\mathbf{r},s) = \begin{cases} \omega_A(\mathbf{r}), & 0 \le s \le f_A/2 \text{ or } f_A/2 < s \le 1\\ \omega_B(\mathbf{r}), & f_A/2 + i(\Delta f_B + \Delta f_C) \le s \le f_A/2 + i(\Delta f_B + \Delta f_C) + \Delta f_B\\ \omega_C(\mathbf{r}), & f_A/2 + j(\Delta f_B + \Delta f_C) + \Delta f_B < s \le f_A/2 + (j+1)(\Delta f_B + \Delta f_C) \end{cases} \quad (6)$$

The initial conditions of eq 5 are $q(r, 0) = 1$ and $q^\dagger(r, 1) = 1$. Equations 2−6 form the basic SCMFT equations. These equations must be solved self-consistently to obtain solutions corresponding to different phases. A comparison of the free energy of these phases can then be used to construct phase diagrams.

There are two main numerical approaches available to solve the SCMFT equations. The first one is the spectral method proposed by Matsen and Schick.[16] In this approach the spatially varying functions are expanded in terms of a set of basis functions, leading to a set of nonlinear algebraic equations. Solving this set of algebraic equations for different phases leads to precise calculation of free energy and phase diagrams.[6,16] Recently it has been demonstrated that the spectral method can be used to discover new ordered phases of complex block copolymers.[7] The second approach of solving the SCMFT is to carry out the computations in real-space. In particular, Drolet and Fredrickson[17] and Bohbot-raviv and Wang[18] have proposed strategies to implement real-space method for SCMFT. It has been demonstrated that the real-space approach can be very useful for the search of new structures. One particular interesting

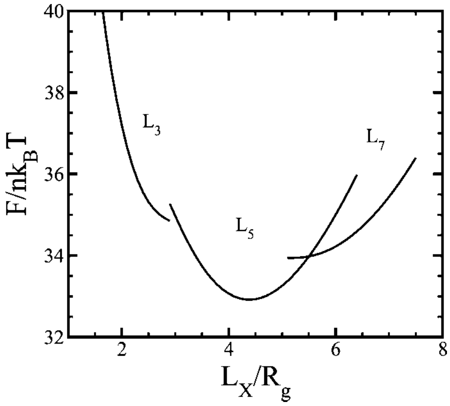

Figure 1. Free energies of L_3, L_5 and L_7 as functions of box size L_x, in unit of R_g, for A(BC)$_4$BA multiblock copolymer with $\chi_{AB}N = \chi_{AC}N = \chi_{BC}N = 200$ and volume fractions $f_A = 0.532$, $f_B = 0.26$, and $f_C = 0.208$. The length of each short block B or C is equal to be 0.052.

example is the studies of confined self-assembly.[19,20] In the present work, we focus on the study of A(BC)$_n$BA multiblock copolymers. A real-space SCFMT method is used to examine the phase diagram of hierarchical lamellar structures with different number of thin-layers formed in A(BC)$_n$BA copolymer. Complementary to the SCMFT calculations, the random phase approximation is used to examine the order–disorder transition of the system.

For the lamellar phases considered in the current study, the system is simplified to be one-dimensional (1D). The split-step fast Fourier transform (FFT) method of Tzeremes et al.[21] is used to solve the modified diffusion equations for $q(\mathbf{r}, s)$ on a $N_x = 512$ lattice. Furthermore, the contour length of each A block is discretized into 256 intervals, whereas the contour lengths of the B and C blocks are divided into 64 interals. Therefore the total contour length of one polymer chain is discretized into $512 + 64 \times (2n + 1)$ intervals. Periodic boundary condition is automatically imposed on the one-dimensional space by the split-step FFT method. Random initial conditions for the mean fields are used to generate a set of lamellar structures with different number of BC-layers. For each lamellar structure with a given number of BC-layers, the free energy is minimized with respect to the box size L_x, which contains one period of the lamellar structure. The equilibrium period of the structure, L_0, corresponds to the box size which minimizes the free energy. By comparing the free energies of these lamellae, the stable equilibrium phase can be identified and the corresponding phase diagram can be constructed.

III. Results and Discussions

For convenience, the heirarchical lamellar structures are labeled as L_k, where k indicates the number of internal BC-layers. In the experiments of ref 9, L_5 is observed in A(BC)$_4$BA melts with $f_A = 0.53$, $f_B = 0.26$, and $f_C = 0.21$. Furthermore, the authors of ref 9 have proposed a mechanism based molecular-configuration counting to explain their observation, The counting model determines that the number of possible molecular-configurations for L_5 is 27, which is larger than the numbers of configurations of the L_3 (15) and L_7 (20). Therefore it can be concluded that L_5 has the largest configuration entropy, justifying its observation in the experiments. In order to test this observation, we compute the free energies of the three lamellae as a function of lamellar period for A(BC)$_4$BA multiblock copolymers. The results are presented in Figure 1. In this calculation, equal repulsive interactions, $\chi_{AB}N = \chi_{AC}N = \chi_{BC}N = 200$, are used. The volume fractions of the different blocks are $f_A = 0.532$, $f_B = 0.26$, and $f_C = 0.208$, which are similar to the values of the experimental system. The effective interaction between two individual B and C blocks is $\chi N(\Delta f_B + \Delta f_C) = 20.8$, which is strong enough to induce BC separation. From the free energy densities plotted in Figure 1, it is obvious that L_5 is the stable phase for A(BC)$_4$BA block copolymer melts. This result is in agreement with the experiments and the simple counting argument for the case of equal repulsive interactions. In the rest of this section, we will show that the SCMFT results reveal structures which are not predicted by the simple counting model when the interaction parameters are changed.

As a first example, we examine the multiblock copolymer A(BC)$_n$BA with $n = 7$. For the A(BC)$_7$BA block copolymers, the configuration numbers for L_5, L_7, and L_9, are 701, 773, and 616, respectively.[9] Because the relative differences between these configuration numbers are smaller, one would expect that L_5 or L_9 structures could become the stable phase in this system. In order to explore this possibility, L_5, L_7 and L_9 structures formed in A(BC)$_7$BA melts are examined. In order to ensure that the equilibrium stable structure is lamellar, the volume fraction of the A blocks is set at $f_A = 0.505$. For simplicity, the B and C block length are set at $\Delta f_B = \Delta f_C = (1 - f_A)/(2n + 1) = 0.033$. The corresponding volume fractions of B and C are $f_B = 0.264$ and $f_C = 0.231$, respectively. Furthermore it is assumed that $\chi_{AB}N = \chi_{AC}N$. In the following paragrams, $\chi_{AB}N$ is used for both $\chi_{AB}N$ and $\chi_{AC}N$.

Starting with random initial conditions, several hierarchical lamellar structures have been obtained. Typical density profiles of these structures are shown in Figure 2. In all of these structures, the number of the BC-layers can only be odd because the number of internal BC blocks is odd. Since the period of these structures depends on the number of internal layers, the box size has to be varied to obtain the equilibrium lamellar phases. For a given lamellar structure, it is important to use a computation box with appropriate box sizes. For example, the structures L_1 and L_3 can only be found in small box sizes. For a given multiblock copolymer architecture, the lamellar structures may be unstable (L_3 and L_7 in Figure 1), metastalbe, or stable (L_5 in Figure 1). Typical free energies of these lamellar phases as a function of the box size L_x are presented in Figure 3. It is can be observed that L_7 is the stable structure with the lowest minimal free energy at its equilibrium period, which is consistent with the simple counting argument. However, it is also observed that L_9 has lower minimal free energy than L_5, which is not consistent with the simple counting argument since L_9 has less configurations than L_5. This result suggests that the simple configuration-counting model can predict the stable lamellar structure in some cases, but can not always tell us which lamellar structure has lower free energy. The reason is that this simple model considers only the contribution of the configurational entropy of the chains to the free energy. Other important contributions include stretching energy and interfacial energy, which are not included in the simple counting model.

We can use the free-energy difference between L_9 and L_7, $\Delta F_{7,9} = F(L_9) - F(L_7)$, to examine the stability of these two structures. When the free-energy difference becomes negative, the L_9 structure becomes a stable structure instead of the L_7 structure. Our results show that the L_9 structure becomes stable when $\chi_{AB}N$ is larger than about 770 for a fixed $\chi_{BC}N = 300$ (Figure 4). This indicates that the stability of these structures can depend on the interactions between the three blocks. The comparison between the two results obtained by two grid sizes of $N_x = 512$ (solid line) and $N_x = 1024$ (symbols) is given in the inset of Figure 4. The consistence suggests that the grid size of $N_x = 512$ gives good accuracy. In order to understand the effects of interaction parameters, we turn to study the influence of $\chi_{BC}N$ on the stability of structures L_7 and L_9. The free-energy difference between L_9 and L_7 is calculated as a function of $\chi_{BC}N$ for a fixed $\chi_{AB}N = 850$ (Figure 5a). When

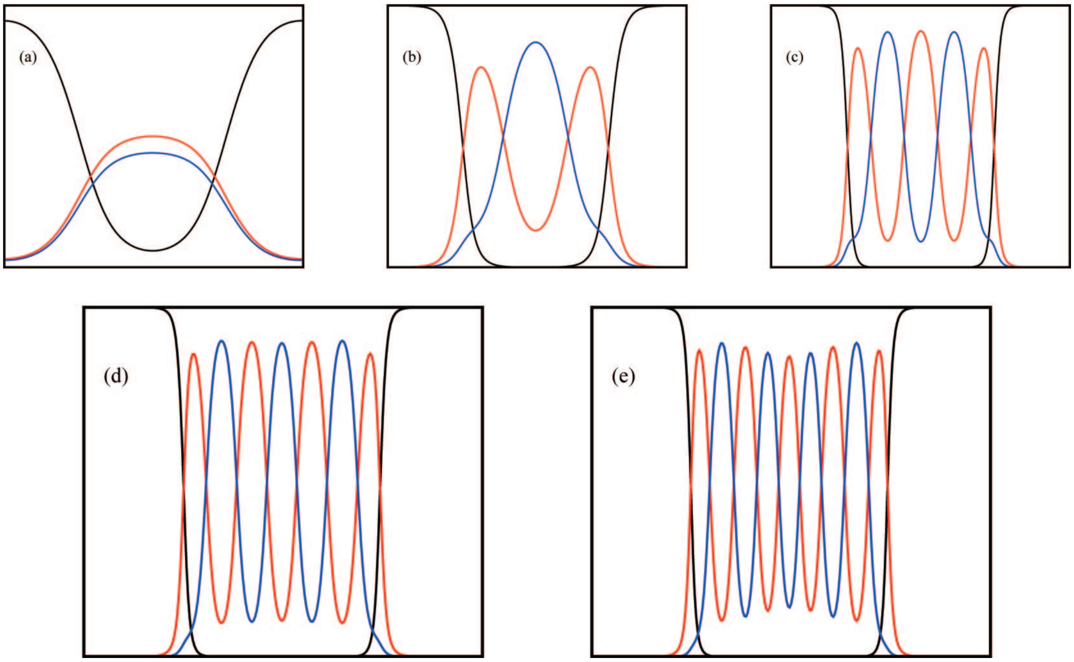

Figure 2. Typical density profiles of hierarchical lamellar structures with number of thin-layers n varying from 1 to 9 for A(BC)$_7$BA multiblock copolymer melts. The compositions of A, B, and C are $f_A = 0.505$, $f_B = 0.264$, and $f_C = 0.231$, respectively. The repulsive interactions are $\chi_{AB}N = \chi_{AC}N = \chi_{BC}N = 300$. These lamellar structures are labeled as L_k, k indicating the number of thin-layers.

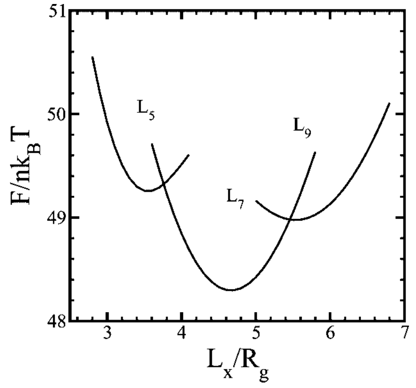

Figure 3. Free energies of L_5, L_7, and L_9 in Figure 2 as functions of box size L_x, in units of R_g.

$\chi_{BC}N$ is smaller than a critical value (about 340), L_9 has lower free energy than L_7. This suggests that it is possible to stabilize L_9 by decreasing $\chi_{BC}N$ for a fixed $\chi_{AB}N$ or by increasing $\chi_{AB}N$ for a fixed $\chi_{BC}N$. Figure 5b shows the periods of lamellar structures L_7 and L_9. It shows that L_9 has larger period than L_7 which is also seen in the similar lamellar structures formed in A(BA)$_n$BA multiblock copolymer melts.[11]

The transition from L_7 to L_9 can be understood from the competition between interfacial energy and chain entropy. The entropy of the multiblock copolymer includes molecular-configurational part and the stretching part. For L_7 and L_9, according to the counting theory in ref 9, L_7 has larger configuration number than L_9. This would be the main factor which makes L_7 more favorable than L_9, if the interfacial energy and chain stretching entropy contributions are equal in these two structures. On the other hand, it is well-known that the AB interfacial energy increases when the interaction parameter χ_{AB} is increased.[22] Larger interfacial energy leads to smaller interfacial area or larger period of the structure, which in turn leads to larger chain stretching energy. One way to release the chain stretching energy is to increase the number of BC layers, so that the B and C stretching is weakened at the cost of increased BC interfacial energy. When χ_{AB} is large enough, it becomes favorable to introduce more BC layers; thus, the L_9 structure becomes stable against the L_7 structure at about $\chi_{AB}N = 770$.

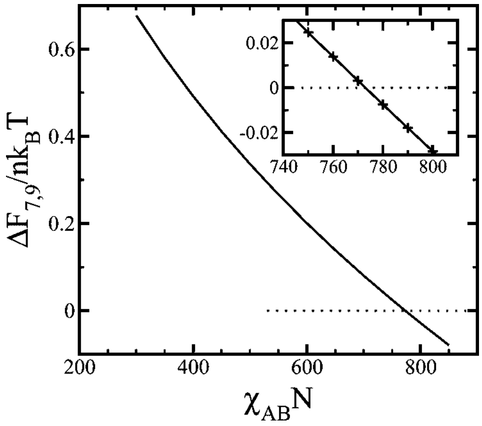

Figure 4. Free-energy difference between L_9 and L_7 for A(BC)$_7$BA with $\chi_{BC}N = 300$ as $\chi_{AB}N = \chi_{AC}N$ varies. The dashed line indicates that the free energy of L_9 is equal to that of L_7. When the difference is positive, it means that L_7 is stable lamellar structure. Othersize L_9 becomes stable structure instead of L_7. The symbols in the inset are obtained with $N_x = 1024$.

If the above argument is correct, one would expect that the L_5 structure may become a stable structure in the opposite limiting case where $\chi_{AB}N$ is much weaker than $\chi_{BC}N$. In addition, the configuration-counting model of ref 9 indicates that L_5 has more possible configurations than L_9. In order to test this possibility, we calculate the free-energy difference between L_5 and L_7, $\Delta F_{7,5} = F(L_5) - F(L_7)$, as a function of $\chi_{BC}N$ for a fixed $\chi_{AB}N = 140$ (Figure 6). For this low value of $\chi_{AB}N = 140$, it is found that $\Delta F_{7,5}$ is negative for a wide range of $\chi_{BC}N$, indicating that L_5 is a stable structure instead of L_7 in this region. The above calculations and analysis clearly demonstrate that different hierarchical lamellar phases can occur in the A(BC)$_n$BA multiblock copolymers. Phase transitions between these structures can be driven by changing the interactions parameters.

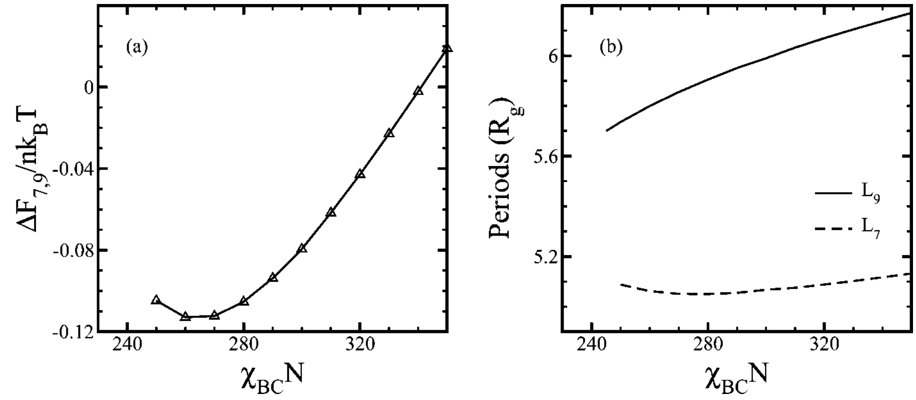

Figure 5. (a) Free-energy difference between L_9 and L_7 for A(BC)$_7$BA with $\chi_{AB}N = \chi_{AC}N = 850$ as $\chi_{BC}N$ varies. (b) Corresponding periods of L_9 (solid line) and L_7 (dashed line).

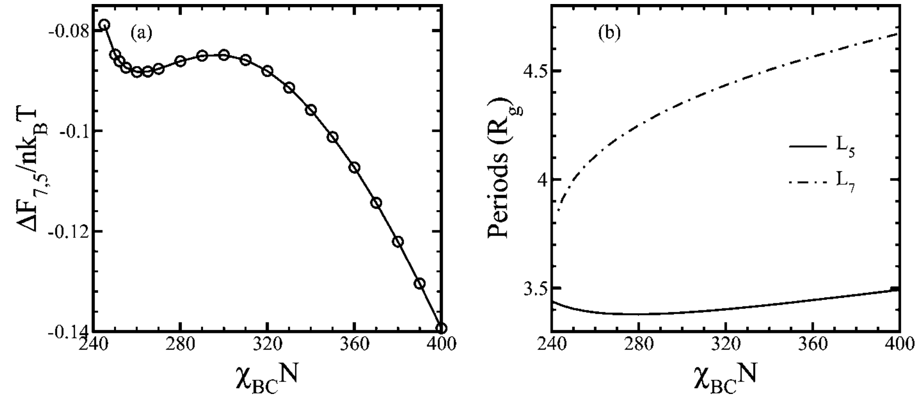

Figure 6. (a) Free-energy difference between L_5 and L_7 for A(BC)$_7$BA with $\chi_{AB}N = \chi_{AC}N = 140$ as $\chi_{BC}N$ varies. (b) Corresponding periods of L_5 (solid line) and L_7 (dashed line).

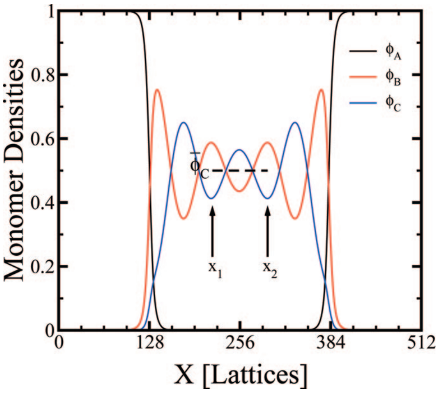

Figure 7. Schematic representation of the definition of an order parameter based on the density profile of C block of L_7. The dashed line indicates the average density of C block, $\bar{\phi}_C$, during the region between two points of x_1 and x_2.

For a given lamellar structure, appearance of the internal BC layers occurs when $\chi_{BC}N$ is large enough. In order to quantitatively determine this transition, we introduce an order parameter to distinguish a hierarchical lamellar phase from the simple lamellar phase in which there is no separation between the B and C blocks. The order parameter based on the hierarchical lamellar structure is defined by

$$\Delta\phi_C = \frac{1}{\bar{\phi}_C}\frac{1}{x_2 - x_1}\int_{x_1}^{x_2} |\phi_C(x) - \bar{\phi}_C|\,\mathrm{d}x, \qquad (7)$$

where $\bar{\phi}_C = 1/(x_2 - x_1)\int_{x_1}^{x_2}\phi_C(x)\,\mathrm{d}x$ is the average density of C block within the region shown in Figure 7. The two end points, x_1 and x_2, are chosen such that the density distribution is not influenced by the A/B interfaces in the interval from x_1 to x_2. A typical order-parameter as a function of $\chi_{BC}N$ at a fixed $\chi_{AB}N = 400$ is given in Figure 8, together with the density profiles of the C block for three values of order parameter ($\Delta\phi_C = 0.56, 0.05, 0.01$). It is seen that in the region of weak segregation (small $\chi_{BC}N$), $\Delta\phi_C$ decreases very slowly, indicating that the occurrence of the internal BC layers might be a crossover, instead of a phase transition. This is reasonable because the BC separation happens in a finite domain, thus no true phase transition is expected. In what follows we will use the criterion that $\Delta\phi_C$ equals to some small number to indicate the transition from a simple lamellar phase to a hierarchical lamellar structure.

The availability of the free energy and order parameter allows us to construct phase diagrams for the A(BC)$_n$BA multiblock copolymers. For the case of A(BC)$_7$BA, the phase diagram in the $\chi_{AB}N - \chi_{BC}N$ space is presented in Figure 9. In this phase diagram, the order-order phase transition boundaries are identified by comparing the free energies between two neighboring structures. The boundary between the disordered phase and ordered phase is calculated using the random phase approximation (RPA) method. Details of RPA for multiblock copolymer A(BC)$_n$BA are given in the Appendix. For a given large value of $\chi_{BC}N > 250$, three hierarchical lamellar phases can be found in the phase diagram. The phase transitions follow the sequence *disorder* → L_5 → L_7 → L_9 when $\chi_{AB}N$ is increased. It is observed that the L_7 phase occupies a large region in the phase diagram, explaining why this structure is the one observed in experiments. The prediction that L_5 and L_9 phases can be stabilized by small and large $\chi_{AB}N$ is a new result. At a given $\chi_{AB}N$ in the L_7 phase region, the BC separation boundary is given in Figure 9 for two different criteria, $\Delta\phi_C = 0.05$ and $\Delta\phi_C = 0.01$. It is clearly seen that this transition is less well defined, reflecting the crossover nature of the process. The order–disorder transition

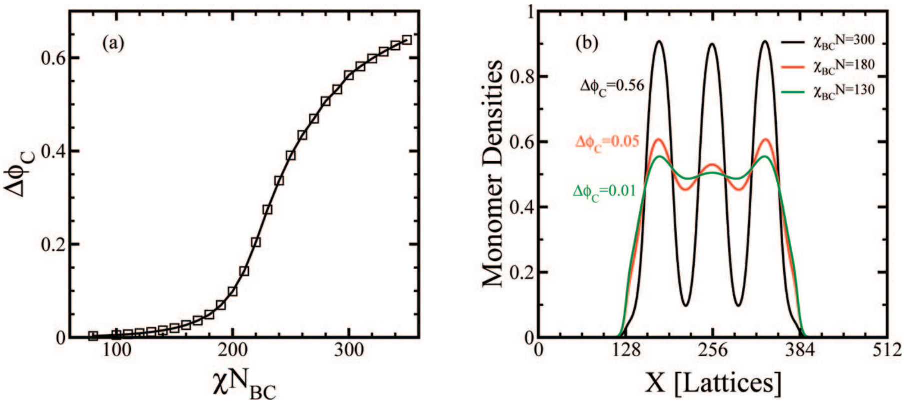

Figure 8. (a) Typical order-parameter function with respect to $\chi_{BC}N$ for $\chi_{AB}N = 400$. (b) Three density profiles of C block for three values of order parameter, $\Delta\phi_C = 0.56$, $\Delta\phi_C = 0.05$, and $\Delta\phi_C = 0.01$, respectively.

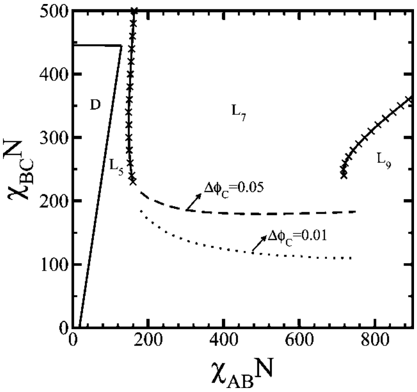

Figure 9. Phase diagram for the stability of lamellar phases L_5, L_7, L_9, and disorder phase D. The region of disorder phase is calculated by random phase approximation method. The points of crosses are identified by scft-consistent mean-field theory, and the lines connected these points are for eye-guide. Dashed line and dotted line indicate two values of order parameter, $\Delta\phi_C = 0.05$ and $\Delta\phi_C = 0.01$, respectively, for the lamellar structure of L_7.

(ODT) boundary is bounded by two limiting cases. At $\chi_{BC}N = 0$, the multiblock becomes ABA triblock copolymer. The ODT in this case is at $\chi_{AB}N \approx 17.96$ for $f_A = 0.505$, and the corresponding ordered structure is simple lamellae without BC segregation. On the other hand, when $\chi_{BC}N \geq 450.0$, B and C blocks start to separate even though the A block is still miscible with B and C blocks. Between these two limiting cases, the ODT moves to larger $\chi_{AB}N$ when $\chi_{BC}N$ is increased.

The above results can be generalized to other multiblock copolymers with different values of n. The phase diagrams for $n = 2$ to $n = 6$ are shown in Figure 10. In these phase diagrams, slightly different volume fractions of the three blocks are used for different number of n: (a) $f_A = 0.5$, $f_B = 0.3$, and $f_C = 0.2$ ($\Delta f_B = \Delta f_C = 0.1$) for $n = 2$; (b) $f_A = 0.51$, $f_B = 0.28$, and $f_C = 0.21$ ($\Delta f_B = \Delta f_C = 0.07$) for $n = 3$; (c) $f_A = 0.532$, $f_B = 0.26$, and $f_C = 0.208$ ($\Delta f_B = \Delta f_C = 0.052$) for $n = 4$; (d) $f_A = 0.505$, $f_B = 0.27$, and $f_C = 0.225$ ($\Delta f_B = \Delta f_C = 0.045$) for $n = 5$; (e) $f_A = 0.506$, $f_B = 0.266$, and $f_C = 0.228$ ($\Delta f_B = \Delta f_C = 0.038$) for $n = 6$. All of these phase diagrams exhibit the same charecteristic as that of the case of $n = 7$, that is, the structure with more BC thin layers is prefered when $\chi_{AB}N$ is increased. For $n = 2$, there are two structures, L_3 and L_5, in the phase diagram. L_3 occupies the region where $\chi_{AB}N$ is lower than or comparable to $\chi_{BC}N$, and L_5 replaces L_3 when $\chi_{AB}N$ is much larger than $\chi_{BC}N$. For the case of $n = 3$, the two main stable ordered phases are L_3 and L_5. This is the same as for the case of $n = 2$, but the transition between L_3 and L_5 is moved toward lower value of $\chi_{AB}N$ than $n = 2$. Therefore the region between the OOT curve and the ODT curve becomes narrower. The trend that the phase region of L_3 decreases from $n = 2$ and $n = 3$ implies that L_3 may not exist in the phase diagram of $n = 4$. Indeed, this is what we found. Specifically, a few OOT points between L_3 and L_5 for $n = 4$ are obtained in the calculations. These points indicate that the phase region of L_3 is tiny. Therefore, in the phase diagram of $n = 4$ of Figure 10c, the OOT curve between L_3 and L_5 is not plotted. For $n = 4$, L_7 appears in the area where $\chi_{AB}N$ is much larger than $\chi_{BC}N$. When n is increased from 4 to 5, L_7 becomes stable when $\chi_{AB}N$ is slightly larger than $\chi_{BC}N$ (see Figure 10d). It is surprising that L_7 is the stable structure instead of L_5 when $\chi_{AB}N$ is smaller than, or comparable with $\chi_{BC}N$ when $n = 6$. For example, L_7 becomes stable when $\chi_{AB}N > 190.7$ for a fixed $\chi_{BC}N = 300$. This result is not consistent with the configuration-counting model, which suggests that the configuration number of L_5, 229, is larger than that of L_7, 218.

Very recently, ten Brinke and co-workers have studied the stability of hierarchical lamellar structures in A(BC)$_n$BA multiblock copolymer melts using strong segregation theory.[12] Contributions to the entropy from different ways of creating specific sequences of loops and bridges are considered. Free energies for different lamellar structures are compared to predict the stable phase. The prediction of their theory is consistent with our SCMFT calculations in that the number of BC-layers depends on the stretching of the individual blocks and the interfacial area. However there are some discrepancies between their predictions and our results. For example, they find stable hierarchical structures for $n = 4$ to $n = 7$ for $\chi_{AB}N = 340$ and $\chi_{BC}N = 85$. From our calculations, the SCMFT predicts a simple lamellar phase with mixed BC layers for the same parameters. The reason for this result is due to the weak BC interactions. Indeed the interactions are $\chi_{BC}N(\Delta f_B + \Delta f_C) = 8.84,\ 7.65,\ 6.46,\ 5.61$ for $n = 4,\ 5,\ 6,\ 7$, which are not strong enough to cause B and C separation. On the other hand, the strong segregation theory assumes that the BC repulsion is very strong. Therefore the strong segregation theory is not applicable to the parameters used in our calculations.

IV. Conclusions

In summary, we have studied the formation of hierarchical lamellar structures in A(BC)$_n$BA multiblock copolymers with $f_A \approx 1/2$. Using real-space self-consistent mean-field theory, we have obtained solutions for several lamellar structures with varied number of BC-layers. The stability of these structures is analyzed by comparing their free energies. It is predicted that more than one lamellar structures are candidates of stable phases besides the predicted stable structure by the simple configuration-counting model.[9] For $n = 7$, the stable structure changes

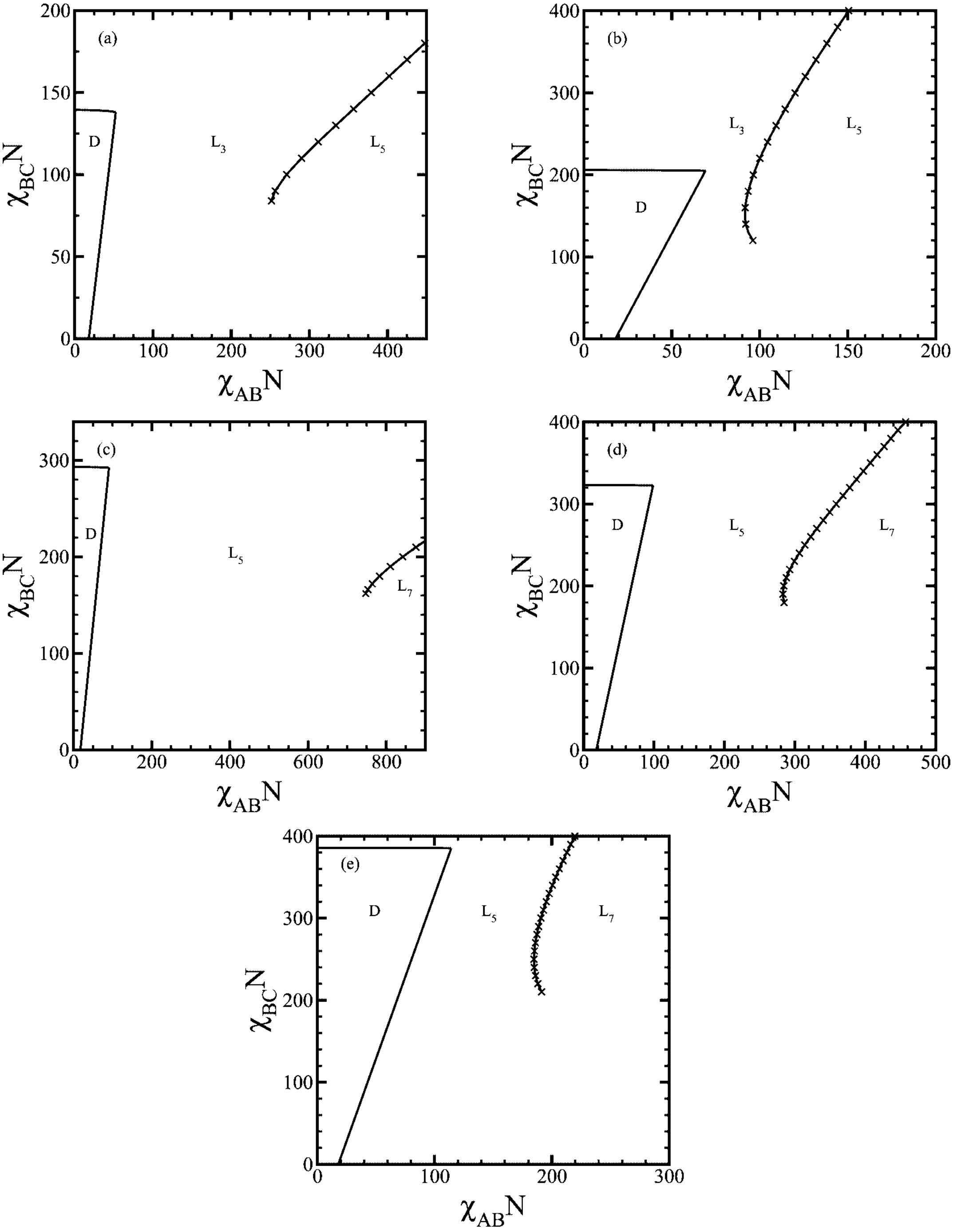

Figure 10. Phase diagrams of multiblock copolymers A(BC)$_n$BA for different repeating number of BC blocks: (a) $n = 2, f_A = 0.5, f_B = 0.3$, and $f_C = 0.2$; (b) $n = 3, f_A = 0.51, f_B = 0.28$, and $f_C = 0.21$; (c) $n = 4, f_A = 0.532, f_B = 0.26$, and $f_C = 0.208$; (d) $n = 5, f_A = 0.505, f_B = 0.27$, and $f_C = 0.225$; (e) $n = 6, f_A = 0.506, f_B = 0.266$, and $f_C = 0.228$.

from L_7 to L_9 when $\chi_{AB}N$ is much stronger than $\chi_{BC}N$. Oppositely, L_5 is preferred than L_7 when $\chi_{AB}N$ is much weaker than $\chi_{BC}N$. In particular, when $n = 6$, our SCMFT results suggest that L_7 is the stable structure instead of L_5 when $\chi_{AB}N$ is smaller than or comparable with $\chi_{BC}N$. This is inconsistent with the prediction of simple configuration-counting model. In addition, random phase approximation method is used to investigate the spinodal from disorder phase to ordered phase. The prediction that the structures with different internal layers can be obtained by tuning the interaction parameters can be useful for the design of block copolymers for these different structures.

Only lamellar phases are considered in the current study. It is expected that nonlamellar BC structures, such as cylinders or spheres in lamellae, could form when the volume fractions of B and C are varied. The formation of these novel phases will be an interesting problem for future studies.

Acknowledgment. The authors would like to thank the Natural Science and Engineering Research Council (NSERC) of Canada for financial support and the SHARCNET and High-end Computing Centre at Fudan University for computing resources. W.L. is supported by the National Natural Science Foundation of China (Grants No. 20704010).

Appendix: Random Phase Approximation

Random phase approximation (RPA), introduced into polymer physics by de Gennes,[23] has been the basis of more elaborate theories for block copolymer melts.[24] The RPA method can be used to determine the spinodal curve of the disordered phase. In what follows, we follow the description of RPA method for ABC triblock copolymer in ref 25 to obtain the main RPA equations. More details can be found in ref 25. In this work, we use RPA method to calculate spinodal values of $(\chi_{ij}N)_{\text{spinodal}}$ $((ij) \in \{(\text{AB}), (\text{AC}), (\text{BC})\})$, where the disorder phase becomes unstable. These values depend on the copolymer composition as well as the architecture of the polymer chains. The collective structure factors, defined as $\tilde{S}_{ij}(\mathbf{q}) \equiv \langle \rho_i(\mathbf{q})\rho_j(-\mathbf{q})\rangle$, first diverge for some wave vector of magnitude q^* when instability occurs. $\rho_i(\mathbf{q})$ is the Fourier form of density $\rho_i(\mathbf{r})$ with average $\langle \rho_i(\mathbf{r})\rangle = f_i$. The state of order or disorder can be described by order parameters defined by

$$\Psi_i(\mathbf{r}) = \langle \rho_i(\mathbf{r}) - f_i \rangle, \tag{8}$$

which vanish in the disorder phase and are spacially periodic funtions in the ordered phases.

The linear set of RPA equations is given by[25]

$$\Psi_i(\mathbf{q}) = -\beta \tilde{S}_{ij}(\mathbf{q}) U_j(\mathbf{q}) = -\beta S_{ij}(\mathbf{q}) U_j^{eff}(\mathbf{q}) \tag{9}$$

$$U_i^{eff}(\mathbf{q}) = U_i(\mathbf{q}) + k_B T \chi_{ik} \Psi_k(\mathbf{q}) + V \tag{10}$$

where $\beta = 1/k_B T$, and V is a chemical potential field that is used as a Lagrange multiplier to impose the condition of incompressiblity on the three order parameter fields. The solution of the above RPA equations takes the form

$$\tilde{S}_{ij}(q) = \frac{F_{ij}(q)}{\Delta(q)}. \tag{11}$$

$F_{ij}(q)$, an expression depending on χ_{ij} and single chain structure factors S_{ij}, can be expressed as

$$\begin{aligned} F_{ii} &= C_{ijk}(q) - 2\chi_{jk} A(q) \\ F_{ij} &= B_{ijk}(q) + A(q)(\chi_{ik} + \chi_{jk} - \chi_{ij}), \end{aligned} \tag{12}$$

where $(ijk) \in \{(\text{ABC}),(\text{BCA}),(\text{CAB})\}$. $\Delta(q)$ can be written as follows:

$$\Delta(q) = S(q) + \sum_{(ijk)} [2\chi_{ij} B_{ijk}(q) - A(q)(\chi_{ij}^{\ 2} - 2\chi_{ij}\chi_{ik})]. \tag{13}$$

Here

$$S(q) = S_{\text{AA}}(q) + S_{\text{BB}}(q) + S_{\text{CC}}(q) + 2[S_{\text{AB}}(q) + S_{\text{BC}}(q) + S_{\text{AC}}(q)] \tag{14}$$

is the total structure factor of a single copolymer chain. The other quantities in eqs 12 and 13 are given by

$$\begin{aligned} A(q) &= S_{\text{AA}}(q) S_{\text{BB}}(q) S_{\text{CC}}(q) + 2 S_{\text{AB}}(q) S_{\text{AC}}(q) S_{\text{BC}}(q) - \\ &\quad [S_{\text{AC}}^{\ 2}(q) S_{\text{BB}}(q) + S_{\text{BC}}^{\ 2}(q) S_{\text{AA}}(q) + S_{\text{AB}}^{\ 2}(q) S_{\text{CC}}(q)] \\ B_{ijk}(q) &= S_{ij}^{\ 2}(q) + S_{ij}(q)[S_{ik}(q) + S_{jk}(q) + S_{kk}(q)] - S_{ii}(q) S_{jj}(q) - \\ &\quad S_{ii}(q) S_{jk}(q) - S_{jj}(q) S_{ik}(q) - S_{ik}(q) S_{jk}(q) \\ C_{ijk} &= S_{ii}(q)[S_{jj}(q) + S_{kk}(q) + 2S_{jk}(q)] - [S_{ij}(q) + S_{ik}(q)]^2. \end{aligned} \tag{15}$$

As we consider the instability of an isotropic disorder phase, the collective structure factors $\tilde{S}_{ij}$ only depend on the magnitude of the wave vector q. Equation 11 indicates that all the $\tilde{S}(q)$ diverge simultaneously, i.e., at the spinodal located by $\Delta(q) = 0$.[25]

Structure factors of a single Gaussian copolymer chain is defined as,[24,25]

$$S_{\alpha\beta}(q) = \frac{1}{N} \sum_{I=1}^{J=N} \Theta_I^{(\alpha)} \Theta_j^{(\beta)} \exp\left(-q^2 \frac{b^2}{6} |I - J|\right), \tag{16}$$

where

$$\Theta_I^{(\alpha)} = \begin{cases} 1 & \text{if } I\text{th monomer is of type } \alpha \\ 0 & \text{otherwise.} \end{cases} \tag{17}$$

The factor $\exp(-q^2(b^2/6)|I - J|)$ gives the statistical weight due to spatial correlations between two points on a strand of Gaussian chain segments with length $|I - J|$. For $\text{A(BC)}_n\text{BA}$ multiblock copolymer, the single-chain structure factors are obtained, by summing expression 16 with respect to I and J along the chain contour, as

$$\begin{aligned} S_{\text{AA}}(q) &= 2N\left(\frac{f_{\text{A}}}{2}\right)^2 \{g(yf_{\text{A}}/2) + [h(yf_{\text{A}}/2)]^2 \exp[-y(1 - f_{\text{A}})]\} \\ S_{\text{BB}}(q) &= N(\Delta f_{\text{B}})^2 \{(n+1) g(y\Delta f_{\text{B}}) + 2[h(y\Delta f_{\text{B}})]^2 \exp(- \\ &\quad y\Delta f_{\text{C}}) \sum_{l=1}^{n+1} \sum_{m=l+1}^{n+1} \exp[-y(m - l - 1)(\Delta f_{\text{B}} + \Delta f_{\text{C}})]\} \\ S_{\text{CC}}(q) &= N(\Delta f_{\text{C}})^2 \{n g(y\Delta f_{\text{C}}) + 2[h(y\Delta f_{\text{C}})]^2 \exp(- \\ &\quad y\Delta f_{\text{B}}) \sum_{l=1}^{n} \sum_{m=l+1}^{n} \exp[-y(m - l - 1)(\Delta f_{\text{B}} + \Delta f_{\text{C}})]\} \\ S_{\text{AB}} &= N f_{\text{A}} \Delta f_{\text{B}} h(yf_{\text{A}}/2) h(y\Delta f_{\text{B}}) \sum_{m=0}^{n} \exp[-my(\Delta f_{\text{B}} + \Delta f_{\text{C}})] \\ S_{\text{AC}} &= N f_{\text{A}} \Delta f_{\text{C}} h(yf_{\text{A}}/2) h(y\Delta f_{\text{C}}) \exp(-y\Delta f_{\text{B}}) \sum_{m=0}^{n-1} \exp[-my(\Delta f_{\text{B}} + \\ &\quad \Delta f_{\text{C}})] \\ S_{\text{BC}} &= N \Delta f_{\text{B}} \Delta f_{\text{C}} h(y\Delta f_{\text{B}}) h(y\Delta f_{\text{C}}) \left\{ \sum_{l=1}^{n} \sum_{m=l}^{n} \exp[-y(m - l)(\Delta f_{\text{B}} + \right. \\ &\quad \left. \Delta f_{\text{C}})] + \sum_{l=2}^{n+1} \sum_{m=1}^{l-1} \exp[-y(l - m - 1)(\Delta f_{\text{B}} + \Delta f_{\text{C}})] \right\}, \end{aligned} \tag{18}$$

where $y = q^2(b^2)/(6)N = q^2 R_g^{\ 2}$, and functions $g(x)$ and $h(x)$ are defined as

$$\begin{aligned} g(x) &= \frac{2}{x^2}[\exp(-x) + x - 1] \\ h(x) &= \frac{1}{x}[1 - \exp(-x)]. \end{aligned} \tag{19}$$

References and Notes

(1) Bates, F. S.; Fredrickson, G. H. *Phys. Today* **1999**, *52*, 32.
(2) Hamley, I. W. *The Physics of Block Copolymers*; Oxford University Press: Oxford, U.K., 1998.
(3) Matsen, M. W.; Bates, F. S. *Macromolecules* **1996**, *29*, 1091.
(4) Abetz, V.; Simon, P. F. W. *Adv. Polym. Sci.* **2005**, *189*, 125.
(5) Matsushita, Y. *Macromolecules* **2007**, *40*, 771.
(6) Tyler, C. A.; Qin, J.; Bates, F. S.; Morse, D. C. *Macromolecules* **2007**, *40*, 4654.
(7) Guo, Z.; Zhang, G.; Qiu, F.; Zhang, D.; Yang, Y.; Shi, A.-C. *Phys. Rev. Lett.* **2008**, *101*, 028301.
(8) Nagata, Y.; Masuda, J.; Noro, A.; Cho, D.; Takano, A.; Matsushita, Y. *Macromolecules* **2005**, *38*, 10220.
(9) Masuda, J.; Takano, A.; Nagata, Y.; Noro, A.; Matsushita, Y. *Phys. Rev. Lett.* **2006**, *97*, 098301.
(10) Nap, R.; Erukhimovich, I.; ten Brinke, G. *Macromolecules* **2004**, *37*, 4296.
(11) Nap, R.; Sushko, N.; Erukhimovich, I.; ten Brinke, G. *Macromolecules* **2006**, *39*, 6765.
(12) Subbotin, A.; Klymko, T.; ten Brinke, G. *Macromolecules* **2007**, *40*, 2915.
(13) Semenov, A. N. *Sov. Phys. JETP* **1985**, *61*, 733.
(14) Shi, A.-C. in *Development in Block Copolymer Science and Technology*; Hamley I. W., Ed.; Wiley: New York, 2004.
(15) Fredrickson, G. H. *The Equilibrium Theory of Inhomogeneous Polymers*; Oxford University Press: Oxford, U.K., 2006.
(16) Matsen, M. W.; Schick, M. *Phys. Rev. Lett.* **1994**, *29*, 1091.
(17) Drolet, F.; Fredrickson, G. H. *Phys. Rev. Lett.* **1999**, *83*, 4317.
(18) Bohbot-Raviv, Y.; Wang, Z. G. *Phys. Rev. Lett.* **2000**, *85*, 3428.
(19) Li, W. H.; Wickham, R. A.; Garbary, R. A. *Macromolecules* **2006**, *39*, 806.
(20) Li, W. H.; Wickham, R. A. *Macromolecules* **2006**, *39*, 8492.

(21) Tzeremes, G.; Rasmussen, K. Ø.; Lookman, T.; Saxena, A. *Phys. Rev. E.* **2002**, *65*−1.

(22) Helfand, E.; Tagami, Y. *J. Polym. Sci., Part B* **1971**, *9*, 741. Helfland, E.; Tagami, Y. *J. Chem. Phys.* **1971**, *56*, 3592.

(23) Gennes, P. G. *Scaling Concepts in Polymer Physics*; Cornell University Press: Ithaca, NY, 1979.

(24) Leibler, L. *Macromolecules* **1980**, *13*, 1602.

(25) Werner, A.; Fredrickson, G. H. *J. Polym. Sci., Part B: Polym. Phys.* **1997**, *35*, 849.

MA801651U